arXiv:0810.0355v1 [physics.atom-ph] 2 Oct 2008

Comparative study of the rovibrational properties of heteronuclear alkali dimers in electric fields

Rosario González-Férez,[1, *] Michael Mayle,[2] Pablo Sánchez-Moreno,[1] and Peter Schmelcher[2, 3]
[1] *Instituto 'Carlos I' de Física Teórica y Computacional and Departamento de Física Atómica Molecular y Nuclear, Universidad de Granada, E-18071 Granada, Spain*
[2] *Theoretische Chemie, Physikalisch–Chemisches Institut, Universität Heidelberg, Im Neuenheimer Feld 229, D-69120 Heidelberg, Germany*
[3] *Physikalisches Institut, Universität Heidelberg, Philosophenweg 12, D-69120 Heidelberg, Germany*

(Dated: October 2, 2008)

A comparative study of the effect of a static homogeneous electric field on the rovibrational spectra of several polar dimers in their $X^1\Sigma^+$ electronic ground state is performed. Focusing upon the rotational ground state within each vibrational band, results for energies and various expectation values are presented. For moderate field strengths the electric field-induced energy shifts, orientation, alignment, and angular motion hybridization are analyzed up to high vibrational excitations close to the dissociation threshold.

PACS numbers: 33.20.-t,32.60.+i,33.20.Vq

INTRODUCTION

The availability of cold and ultracold dimers provides a unique opportunity to investigate fundamental quantum processes [1]. The efforts of many experimental groups are focused on the production of heteronuclear alkali dimers, as they constitute a prototype of an ultracold quantum gas with long-range dipole-dipole interactions. In this context, the photoassociation of LiCs, NaCs, KRb, and RbCs has been reported recently [2, 3, 4, 5], while Feshbach resonances have been observed for LiNa, LiK, LiRb, and KRb [6, 7, 8, 9, 10]. The long-range anisotropic dipole-dipole interaction between these polar molecules gives rise to an intriguing many body physics with new interesting physical phenomena. In addition, these systems allow for a wide range of applications, such as state resolved chemical reactions [11] or quantum computing [12, 13].

Particularly interesting is the study of the influence of external fields on these molecular systems. External fields play a key role in trapping and cooling processes as well as in the manipulation and control of the dipole-dipole interaction, chemical reactions or collisions [14]. As an example, the application of an electric field has been predicted to significantly affect the photoassociation process of ultracold polar molecules as well as the subsequent radiative decay cascade [15, 16]. On the other hand, the internal structure of molecules is significantly affected by an electric field. The strong field regime is characterized by the appearance of pendular states: The molecule is oriented along the field axis and can be described as a coherent superposition of field-free rotational states. Recently, the authors have performed studies of the rovibrational spectra of CO and LiCs in their electronic ground states exposed to an electric field: The orientation and hybridization of the angular motion, the Stark shift, and the radiative decay properties have been investigated for a wide range of field strengths and rovibrational levels [17, 18, 19]. In the present work we extend our previous studies by performing a comparative analysis of several polar alkali dimers which are of immediate experimental interest. Specifically, we analyze the influence of a static electric field on the $X^1\Sigma^+$ electronic ground state of ^{6}Li^{23}Na, ^{6}Li^{40}K, ^{6}Li^{87}Rb, ^{7}Li^{133}Cs, ^{23}Na^{39}K, ^{23}Na^{133}Cs, ^{39}K^{85}Rb, and ^{85}Rb^{133}Cs.

ROVIBRATIONAL HAMILTONIAN

In the following we consider the field regime where perturbation theory holds for the description of the molecular electronic structure. The Born-Oppenheimer approach then provides the following Hamiltonian for the nuclear motion of a polar dimer in its electronic ground state exposed to a static electric field

$$H = T_R + \frac{\hbar^2 \mathbf{J}^2(\theta,\phi)}{2\mu R^2} + \varepsilon(R) - FD(R)\cos\theta \qquad (1)$$

where the molecule fixed frame with the origin at the center of mass of the nuclei has been employed, (R, θ, ϕ) being the internuclear distance and the Euler angles[33]. T_R, μ, $\hbar\mathbf{J}(\theta,\phi)$, $\varepsilon(R)$, and $D(R)$ are the vibrational kinetic energy, the reduced mass of the nuclei, the rotational angular momentum, the field-free electronic potential energy curve (PEC), and the electronic dipole moment function (EDMF), respectively. The electric field is taken parallel to the laboratory frame z-axis with strength F. Since we restrict ourselves on a nonrelativistic treatment, couplings to electronic states of different spin symmetry do not arise.

In the framework of the effective rotor approach [17], the rovibrational Hamiltonian (1) reduces to

$$H_\nu^{ERA} = \frac{\hbar^2}{2\mu}\langle R^{-2}\rangle_\nu^0 \mathbf{J}^2 - F\langle D(R)\rangle_\nu^0 \cos\theta + E_\nu^0 \qquad (2)$$

with $\langle R^{-2}\rangle_\nu^0 = \langle\psi_\nu^0|R^{-2}|\psi_\nu^0\rangle$, $\langle D(R)\rangle_\nu^0 = \langle\psi_\nu^0|D(R)|\psi_\nu^0\rangle$. ψ_ν^0 and E_ν^0 are the field-free vibrational wave function and energy for a given vibrational state ν with $J = 0$, respectively. This approximation, which is valid for large parts of the rovibrational spectrum, relies on two assumptions: i) the rotational and vibrational energy scales should differ by several orders of magnitude and can therefore be separated adiabatically, and ii) the field influence on the vibrational motion is very small and can consequently be treated by perturbation theory. Besides reducing (1) to an one-dimensional problem, this approach allows us to compare the field influence on several vibrational levels, and even between different molecular species, by means of the parameter

$$\omega_\nu = \frac{2\mu\langle D(R)\rangle_\nu^0}{\hbar^2\langle R^{-2}\rangle_\nu^0}, \qquad (3)$$

which derives from rescaling the Hamiltonian (2) using the rotational constant of a given vibrational state, $B_\nu = \hbar^2\langle R^{-2}\rangle_\nu^0/2\mu$. If $\omega_\nu \cdot F$ acquires the same order of magnitude as the rescaled rotational kinetic energy, $\mathbf{J}^2$, the rotational dynamics is severely altered by the interaction with the electric field, while ω_ν^{-1} provides an estimation of the field strength needed to show a significant effect.

We remark that in the presence of the electric field, only the magnetic quantum number is retained, whereas the vibrational and rotational ones are no more conserved. However, for reasons of addressability, we will label the electrically dressed states by means of their field-free vibrational, rotational, and magnetic quantum numbers (ν, J, M). Furthermore, in this letter we focus on rotationally non-excited states with corresponding field-free quantum numbers $J = M = 0$. The computational method used to solve the full rovibrational Schrödinger equation is described in ref. [17].

ELECTRONIC POTENTIAL CURVES AND DIPOLE MOMENT FUNCTIONS

The PECs of the singlet electronic ground states of the alkali dimers employed here are derived from either experimental or theoretical studies. For the PECs of LiNa, LiK, LiCs, NaK, NaCs, KRb, and RbCs we use very accurate experimental data from spectroscopic analyses [20, 21, 22, 23, 24, 25, 26]. The LiRb PEC is taken from theoretical studies based on a semiempirical method [27]. When describing vibrationally highly excited states, special attention has to be payed to the long-range part of the PECs: For LiNa, LiCs, NaCs, KRb, and RbCs, the PECs include van der Waals terms, $-\sum_{n=6,8,10} C_n/R^n$, and an exchange energy term, $-AR^\gamma e^{-\beta R}$, see refs. [20, 21, 22, 24, 25, 26], with $\gamma = 0$ for LiNa [21]. The long-range part of the NaK PEC additionally includes damping functions $\xi_n(R)$ in the van der Waals expansion, $-\sum_{n=6,8,10}\xi_n(R)C_n/R^n$, and a different expression for the exchange energy, $-Ae^{-\alpha R-\beta R^2}$ [23]. For the LiRb dimer only the first van der Waals term, $-C_6/R^6$, is considered [28].

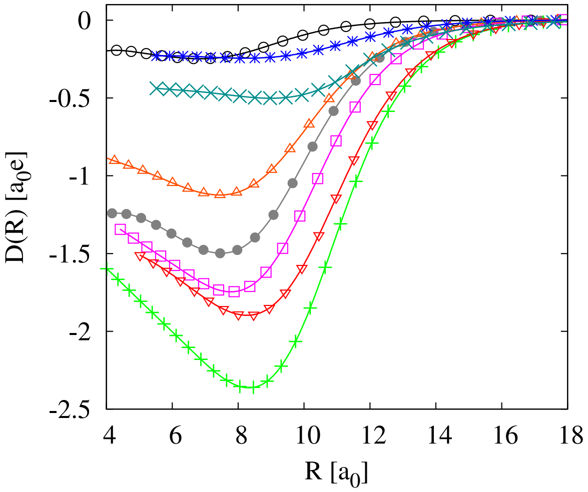

FIG. 1: Color online. Electric dipole moment functions of the $X\,^1\Sigma^+$ electronic ground states of LiNa (○), LiK (●), LiRb (□), LiCs (+), NaK (△), NaCs(▽), KRb (∗), and RbCs (×).

The EDMFs employed for the LiNa, LiK, LiCs, NaK, NaCs, and KRb systems are computed by the same semiempirical technique as the LiRb PEC [29]. The RbCs EDMF is taken from an ab-initio relativistic valence-bound calculation [30]. Since for the electronic ground state of the polar alkali dimers the long-range behaviour of the EDMF is given by D_7/R^7 [31], this asymptotic function has been fitted to the theoretical data at large internuclear distances. We note that, when necessary for computational reasons, the short-range behaviour of the EDMFs is linearly extrapolated. The resulting EDMFs are plotted in fig. 1 as a function of the internuclear distance. All EDMFs are negative and exhibit a broad minimum which is shifted with respect to the minimum of the corresponding PEC, *e.g.*, by 0.51 and $1.39\,a_0$ for the KRb and LiCs dimers, respectively. The EDMFs of LiRb, NaK, NaCs, and KRb become positive for $R \gtrsim 17.3\,a_0$ albeit approaching zero thereafter; this change of sign will be reflected in the response of highly excited rovibrational levels to the field. However, this has to be taken with a grain of salt since ab-initio electronic structure calculations of molecules typically employ basis sets of exponentially localized functions, which do not easily catch the long-range behaviour of the atom-atom interaction. The LiCs EDMF has the largest absolute value with a maximum of $|D(R)| = 2.36\,a_0e$ at

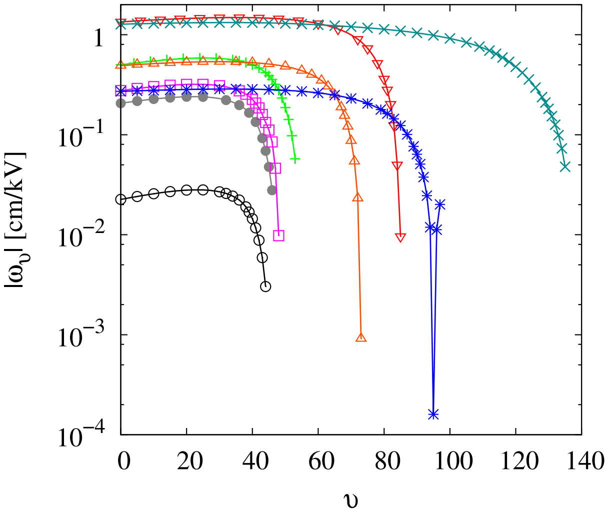

FIG. 2: Color online. The parameter $|\omega_\nu|$ versus the field-free vibrational quantum number ν for the same dimers as in fig. 1.

$R = 8.3\,a_0$. The EDMFs of LiNa, KRb, and RbCs show only a weak dependence on R for a wide range of internuclear distances and overall comparatively small values for the dipole moment.

RESULTS

Let us start by analyzing the behaviour of the parameter ω_ν as a function of the vibrational quantum number. In fig. 2, the modulus of ω_ν is presented for the $(\nu, 0, 0)$ levels of all dimers on a logarithmic scale. The maximum vibrational quantum numbers considered are $\nu = 44$ (LiK), 46 (LiNa), 48 (LiRb), 53 (LiCs), 73 (NaK), 85 (NaCs), 97 (KRb), and 135 (RbCs); the very last vibrational bands have not been included. For all dimers, $|\omega_\nu|$ shows a qualitatively similar but quantitatively different behaviour as a function of ν: After a weakly pronounced maximum, $|\omega_\nu|$ decreases rapidly for high vibrational excitations. In particular, NaK, KRb, and RbCs show a plateau-like behaviour indicating a quantitatively similar field impact in many vibrational bands. According to their $|\omega_\nu|$ values, the considered molecules can be classified into four groups whose response to the field will be of comparable magnitude for a large part of their spectra. Possessing the largest $|\omega_\nu|$ values, the first group is formed by the NaCs and RbCs dimers and their $\nu \lesssim 65$ states, followed by the $\nu \lesssim 40$ levels of LiCs and NaK. Despite the large LiCs EDMF, the corresponding $|\omega_\nu|$ is only approximately half of the $|\omega_\nu|$ belonging to NaCs and RbCs: The large reduced masses of the latter compensate their smaller dipole moments. The third set contains LiK, LiRb, and KRb and their lowest 40 vibrational bands. Finally, LiNa will be least affected by the field which is due to both small $D(R)$ and μ. We remark that the sign of ω_ν depends crucially on the corresponding dipole moment: While being generally negative, the change of sign of the NaK, NaCs, and KRb EDMFs at long distances causes $\omega_\nu > 0$ for their $\nu \geq 73$, 85 and 95 levels, respectively. In particular, the minimum observed for the $\nu = 95$ level of KRb can be attributed to this change of sign. For all molecules considered, the slope of $|\omega_\nu|$ becomes very steep as ν approaches the dissociation threshold. Consequently $|\omega_\nu|$ drastically varies from its maximum to its minimum; for example we get for LiNa $\omega_{26} = -2.8 \times 10^{-2}$ versus $\omega_{46} = -3.0 \times 10^{-3}$ cm/kV, and for NaCs $\omega_{35} = -1.49$ versus $\omega_{85} = -9.6 \times 10^{-3}$ cm/kV. Hence, for high-lying vibrational excitations the field strength should be enhanced at least one order of magnitude to obtain similar field-dressed states as on the lower part of the rovibrational spectrum.

In order to quantify the spectral changes upon the application of the electric field, we consider the ratio of the Stark shift to the rotational spacing in the presence of the field

$$\kappa_\nu = \frac{E_{\nu 0}(0) - E_{\nu 0}(F)}{E_{\nu 1}(F) - E_{\nu 0}(F)} \tag{4}$$

where $E_{\nu 0}(F)$ and $E_{\nu 1}(F)$ are the energies of the $(\nu, 0, 0)$ and $(\nu, 1, 0)$ levels at field strength F; for high-field seekers we get $\kappa_\nu > 0$. If $\kappa_\nu \ll 1$, the field-dressed spectrum shows many similarities to the field-free one. In particular, this criterion is fulfilled for $\omega_\nu F \ll 1$: In second order perturbation theory the $(\nu, 0, 0)$ and $(\nu, 1, 0)$ states are shifted by $-\omega_\nu^2 F^2 B_\nu/6$ and $\omega_\nu^2 F^2 B_\nu/6$ [32], respectively, compared to the field-free rotational spacing of $2B_\nu$.

In figs. 3(a) and (b) the parameter κ_ν is presented as a function of the vibrational quantum number for $F = 5.14$ and 51.4 kV/cm, respectively; the selected field strengths are chosen such that the experimentally accessible range within the strong field regime is covered. Besides showing high-field seeking character, the behaviour of κ_ν has many analogies among the considered molecules. Initially, it has a weak dependence on the vibrational excitation, thereby smoothly increasing as ν is enhanced and passing a shallow maximum (due to the semilogarithmic scale, this increasing trend appears as a plateau). For higher vibrational excitations, κ_ν rapidly decreases as the levels get closer to the dissociation limit: This reduction can be up to one order of magnitude when ν is enhanced by merely one quantum. The above classification of the considered molecules is equally observed for κ_ν. The lowest values appear for LiNa, $\kappa_\nu \leq 2 \times 10^{-3}$ and 0.2, for $F = 5.14$ and 51.4 kV/cm, respectively, *i.e.*, the impact of the field on the spectrum is negligible for the smaller of these two field strengths. In contrast, NaCs and RbCs are most affected by the field $F = 5.14$ kV/cm, with $\kappa_\nu > 0.5$ for $\nu \leq 68$ and 89, respectively. LiCs and NaK possess values $\kappa_\nu > 0.2$ for $\nu \leq 44$ and 58, respectively. For LiRb and KRb we found $\kappa_\nu > 0.1$ for the $\nu \leq 38$

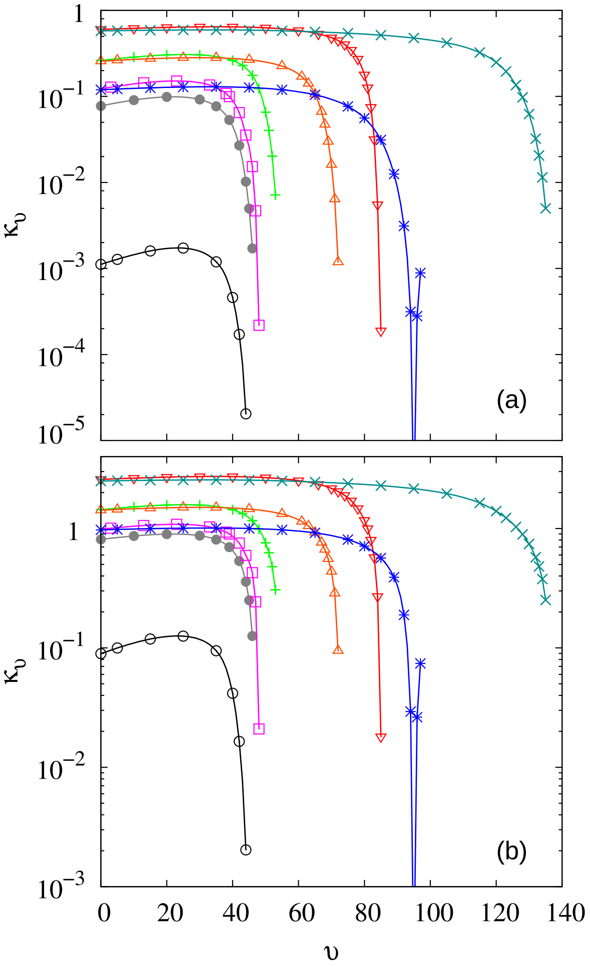

FIG. 3: Color online. The relative energy shift κ_ν as a function of the field-free vibrational quantum number for the $(\nu, 0, 0)$ levels and same molecules as in fig. 1, for (a) $F = 5.14$ kV/cm and (b) 51.4 kV/cm.

and 67 states, whereas a smaller value is achieved for LiK with $\kappa_\nu > 0.08$ for $\nu \leq 34$. An increase of the field strength by one order of magnitude ($F = 51.4$ kV/cm) produces a significant variation of κ_ν, which depends on the system and especially on the states under consideration. Indeed, we observe $\kappa_\nu > 1$ for most levels of LiCs, NaK, NaCs, and RbCs. The levels $\nu \leq 36, 41$, and 75 of LiK, LiRb, and KRb satisfy $\kappa_\nu > 0.8$. In order to provide a reasonable scaling, the minimum of κ_ν for KRb at $\nu = 95$ has not been included in fig. 3.

The orientation and alignment of the pendular states are characterized by the expectation value $\langle\cos\theta\rangle$ and $\Delta\cos\theta = \sqrt{\langle\cos^2\theta\rangle - \langle\cos\theta\rangle^2}$, respectively. The closer $\Delta\cos\theta$ is to zero, the stronger is the alignment and the closer the modulus of $\langle\cos\theta\rangle$ is to one, the stronger is the orientation of the state along the field. The expectation value $\langle\cos\theta\rangle$ of these levels is presented in figs. 4(a) and (b) for $F = 5.14$ and 51.4 kV/cm, respectively, as a function of the field-free vibrational quantum number. The corresponding results for $\Delta\cos\theta$ are shown in figs. 5(a) and (b). The sign of the effective electric dipole moment, $\langle D(R)\rangle_\nu^0$, determines whether the orientation will be parallel or antiparallel to the field direction, *i.e.*, $\langle\cos\theta\rangle > 0$ or $\langle\cos\theta\rangle < 0$, respectively.

For the moment let us focus on the description of the results for $F = 5.14$ kV/cm, see figs. 4(a) and 5(a). As expected from the behaviour of the parameter ω_ν, the orientation smoothly increases as ν is enhanced, reaching a broad maximum and rapidly decreasing thereafter as the state gets close to the dissociation threshold. Since the initial increasing trend is not very pronounced for NaK, NaCs, KRb, and RbCs, $\langle\cos\theta\rangle$ exhibits a plateau as a function of ν followed by a rapid decrease of the orientation. The strongest orientation is achieved for the NaCs and RbCs dimers with $\langle\cos\theta\rangle \leq -0.7071$, for the $\nu \leq 65$ and 76 levels, respectively. The states $\nu \leq 44$ and 56 of LiCs and NaK, respectively, present a significant orientation as well: $\langle\cos\theta\rangle \lesssim -0.5$. For LiK, LiRb, and KRb the influence of the field is not very pronounced and the extremal values are $\langle\cos\theta\rangle = -0.35$, -0.43, and -0.40 for the $\nu = 22$, 23, and 33 levels, respectively. For LiNa as well as for highly vibrationally excited levels of the other molecules, the effect of an electric field of strength $F = 5.14$ kV/cm is negligible. Analogous conclusions are derived from the analysis of $\Delta\cos\theta$, whose behaviour as a function of ν is very similar to the one previously described for $\langle\cos\theta\rangle$. The variation of $\Delta\cos\theta$ is very smooth as ν is augmented, and major changes are observed only for high-lying excitations. The NaCs and RbCs dimers show the strongest alignment, with $\Delta\cos\theta < 0.3$ for the $\nu \leq 72$ and 99 levels, respectively. The other dimers present relative large values with $\Delta\cos\theta > 0.3703$ which is the lowest one achieved for LiCs at $\nu = 25$, indicating a modest alignment. In particular, $\Delta\cos\theta$ is very close to its field-free value, *i.e.*, $\Delta\cos\theta \approx 0.577$, for the LiNa dimer and for all high-lying vibrational levels.

If the field strength is increased to $F = 51.4$ kV/cm, both the orientation and alignment are more pronounced, see figs. 4(b) and 5(b). Except for the LiNa molecule, the strong field regime with the appearance of pendular states is already reached for most of the levels considered. We observe $\langle\cos\theta\rangle \lesssim -0.8$ for the states with $\nu \leq 38, 48, 65, 81$, and 108 of the LiRb, LiCs, NaK, NaCs, and RbCs dimers, respectively. Even more, $\langle\cos\theta\rangle \lesssim -0.9$ for the $\nu \leq 70$ and 96 states of NaCs and RbCs, respectively. The LiNa molecule still shows a modest orientation, with a minimal value $\langle\cos\theta\rangle = -0.394$ for the $\nu = 23$ state: only if F is further increased by one order of magnitude a significant orientation, *i.e.*, $\langle\cos\theta\rangle \lesssim -0.8$, is attained for this molecule. For $F = 51.4$ kV/cm, the strong field regime is also manifest in $\Delta\cos\theta$ where many levels present a pronounced alignment with $\Delta\cos\theta < 0.3$. The smallest values, $\Delta\cos\theta \lesssim 0.1$, are obtained for the $\nu \leq 71$ and 100 states of NaCs and RbCs, respectively. In

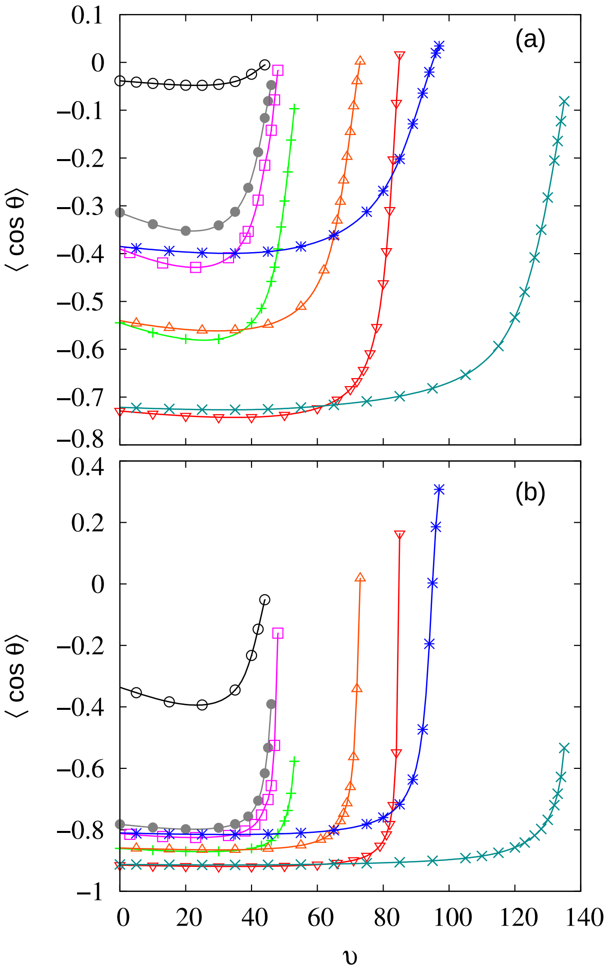

FIG. 4: Color online. The same as fig. 3 but for the expectation value $\langle\cos\theta\rangle$.

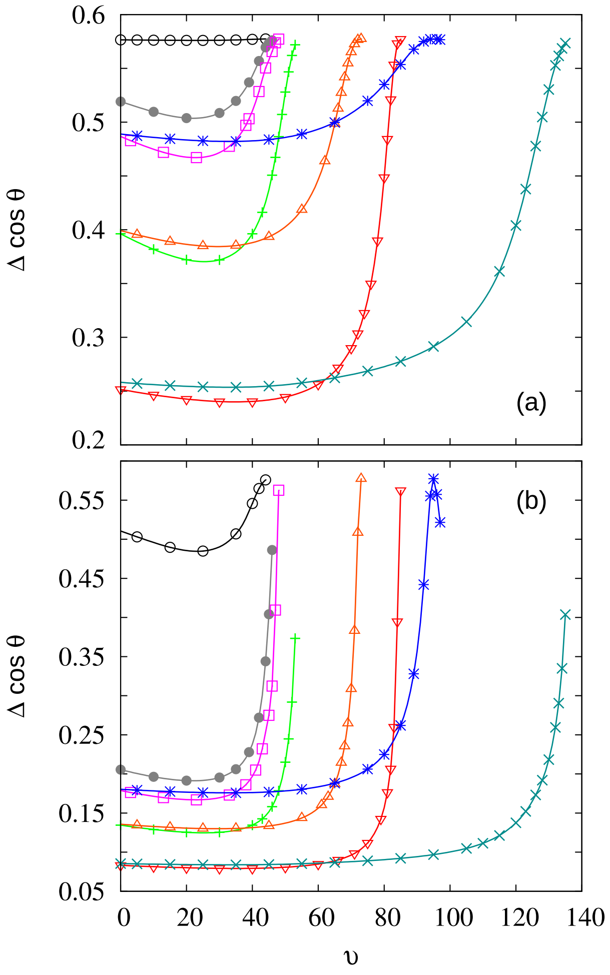

FIG. 5: Color online. The same as fig. 3 but for $\Delta\cos\theta$.

contrast, for the LiNa dimer we find that $\Delta\cos\theta \gtrsim 0.485$ for any ν. Finally, let us remark that $\langle\cos\theta\rangle$ is positive for the states with $\nu \geq 73$, 85, and 95 of the NaK, NaCs, and KRb dimers, respectively, while being characterized by a weak orientation and alignment at both field strengths. In particular, for KRb $|\langle\cos\theta\rangle|$ ($\Delta\cos\theta$) achieves a minimum (maximum) for the $\nu = 95$ level, *i.e.*, for the same state as $|\omega_\nu|$ shows a minimum, cf. fig. 2.

The expectation value $\langle\mathbf{J}^2\rangle$ provides an estimate of the field-induced hybridization of the angular motion. Since we only consider the rotational ground state in this letter, one yields $\langle\mathbf{J}^2\rangle = 0$ for $F = 0$. Figures 6(a) and (b) illustrate the evolution of $\langle\mathbf{J}^2\rangle$ with increasing degree of vibrational excitation for $F = 5.14$ and 51.4 kV/cm, respectively. For both field strengths investigated, $\langle\mathbf{J}^2\rangle$ presents a similar behaviour for all molecules: It increases as the vibrational excitation is enhanced, passes through a broad maximum, and decreases, approaching zero, thereafter. The lower parts of the NaK, KRb, and RbCs spectra show again a plateau-like behaviour of $\langle\mathbf{J}^2\rangle$. For $F = 5.14$ kV/cm, the rotational dynamics has mostly s-wave character, *e.g.*, 47% for the $\nu = 34$ level of NaCs, 73% for the $\nu = 29$ state of NaK, and 87% for the $\nu = 33$ level of KRb. The hybridization of the angular motion is negligible for LiNa, *i.e.*, $\langle\mathbf{J}^2\rangle < 3.5\times10^{-3}\,\hbar^2$ for any ν, and 99.8% of the dynamics is controlled by the $J = 0$ wave. In contrast, the pendular character of the NaCs and RbCs dimers is already significant with $\langle\mathbf{J}^2\rangle > 1.0\,\hbar^2$ for the $\nu \leq 71$ and 98 levels, respectively. The $\nu \leq 42$ and 52 states of LiCs and NaK, respectively, satisfy $\langle\mathbf{J}^2\rangle > 0.5\,\hbar^2$; analogously we observe for LiRb and KRb $\langle\mathbf{J}^2\rangle > 0.2\,\hbar^2$ for $\nu \leq 39$ and 67. For the LiK states we find $\langle\mathbf{J}^2\rangle > 0.15\,\hbar^2$ for $\nu \leq 35$.

Because of the high-field seeking character of these levels, $\langle\mathbf{J}^2\rangle$ is drastically increased for $F = 51.4$ kV/cm, see fig. 6(b). Except for LiNa, strong field effects characterize this expectation value for a wide range of levels. Indeed, $\langle\mathbf{J}^2\rangle > 5.0\,\hbar^2$ for the $\nu \leq 64$ and 73 states of NaCs and RbCs, $\langle\mathbf{J}^2\rangle > 3.0\,\hbar^2$ for those with $\nu \leq 50$ and 41 of the NaK and LiCs dimers, and $\langle\mathbf{J}^2\rangle > 1.8\,\hbar^2$ for the lowest 35 vibrational states of LiK. They present a rich pendular dynamics, with significant contributions of higher field-free rotational states. As ν gets closer to

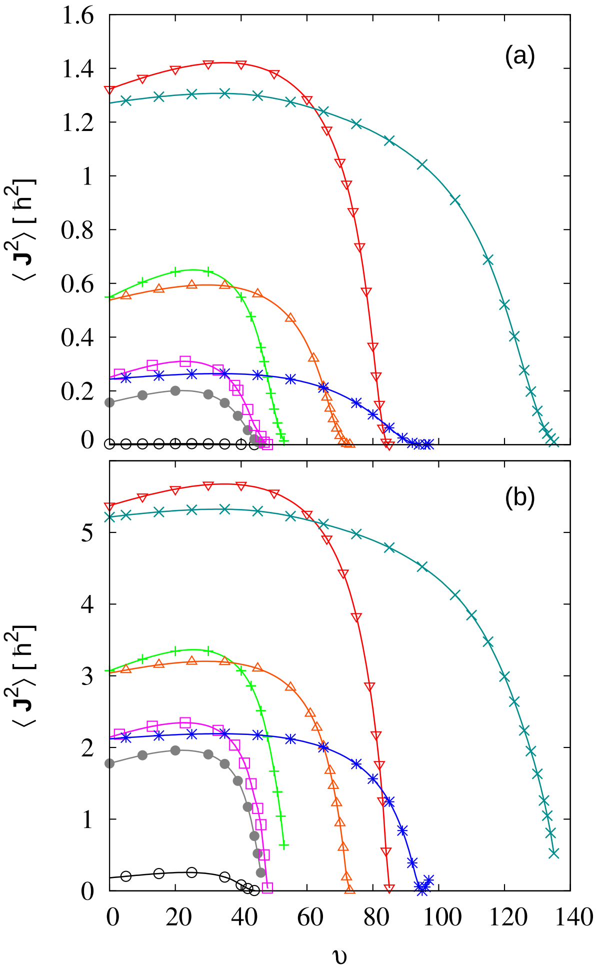

FIG. 6: Color online. The same as fig. 3 but for the expectation value $\langle \mathbf{J}^2 \rangle$.

the dissociation limit the relative weight of the s-wave becomes more important, and $\langle \mathbf{J}^2 \rangle$ is reduced. In contrast, the field-free $J = 0$ level still dominates the LiNa states with $\langle \mathbf{J}^2 \rangle < 0.26\,\hbar^2$ for any ν-value. Finally, let us remark that the effect of the field in terms of $\langle \mathbf{J}^2 \rangle$ for the $\nu = 95$ level of KRb is negligible but slightly increases again for the last states.

CONCLUSION

In conclusion, we have investigated the rovibrational spectra of the electronic ground state $\mathrm{X}^1\Sigma^+$ of the alkali dimers LiNa, LiK, LiRb, LiCs, NaK, NaCs, KRb, and RbCs in the presence of a static homogeneous electric field. Performing a comparative analysis, we have considered the lowest rotational excitation within each vibrational band up to the dissociation limit. The vibrational state-dependent parameter ω_ν provides a first estimation of the influence of the field on the corresponding dimer and allows a classification of these systems into four groups. Thus, NaCs and RbCs are most affected by the application of an electric field and LiNa is least. In general, vibrationally highly excited states show less field impact whereas already for moderate field strengths pronounced effects are observed for lower-lying levels. The richness and variety of field-dressed rotational dynamics have been illustrated by analyzing the Stark shift of the spectra as well as the orientation, alignment, and hybridization of the angular motion.

This work should serve as a guide to experimentalists interested in electric field effects on cold and ultracold heteronuclear alkali dimers. A natural extension of this work includes the study of the influence of the field on states emerging from higher rotational excitations and/or with nonzero magnetic quantum numbers M.

Financial support by the Spanish projects FIS2005–00973 (MEC) and FQM–0207, FQM–481 and P06-FQM-01735 (Junta de Andalucía) is gratefully appreciated.

---

[*] Electronic address: rogonzal@ugr.es

[1] Topical Issue on Ultracold Polar Molecules: Formation and Collisions, Eur. Phys. J. D **31**
[2] Kraft S. D. *et al.*, J. Phys. B **39**, S993 (2006)
[3] Haimberger C. *et al.*, Phys. Rev. A **70**, 021402(R) (2004)
[4] Wang D. *et al.*, Eur. Phys. J. D **31**, 165 (2004)
[5] Sage J. M. *et al.*, Phys. Rev. Lett. **94**, 203001 (2005)
[6] Stan C. A. *et al.*, Phys. Rev. Lett. **93**, 143001 (2004)
[7] Deh B. *et al.*, Phys. Rev. A **77**, 010701(R) (2008)
[8] Wille E. *et al.*, Phys. Rev. Lett **100**, 053201 (2008)
[9] Hodby E. *et al.*, Phys. Rev. Lett **94**, 120402 (2005)
[10] Ospelkaus S. *et al.*, Phys. Rev. Lett **97**, 120402 (2006)
[11] Bodo E., Gianturco F. A. Dalgarno A., J. Phys. B **35**, 2391 (2002)
[12] DeMille D., Phys. Rev. Lett. **88**, 067901 (2002)
[13] Yelin S. F., Kirby K. Côté R., Phys. Rev. A **74**, 050301(R) (2006)
[14] Krems R. V., Phys. Rev. Lett. **96**, 123202 (2006)
[15] González-Férez R., Mayle M. Schmelcher P., Europhys. Lett. **78**, 53001 (2007)
[16] González-Férez R., Weidemüller M. Schmelcher P., Phys. Rev. A. **76**, 023402 (2007)
[17] González-Férez R. Schmelcher P., Phys. Rev. A **69**, 023402 (2004)
[18] González-Férez R., Mayle M. Schmelcher P., Chem. Phys. **329**, 203 (2006)
[19] Mayle M., González-Férez R. Schmelcher P., Phys. Rev. A **75**, 013421 (2007)
[20] Martin F. *et al.*, J. Chem. Phys. **115**, 4118 (2001)
[21] Fellows C. E., J. Chem. Phys. **94**, 5855 (1991)
[22] Staanum P. *et al.*, Phys. Rev. A **75**, 042513 (2007)
[23] Russier-Antoine I. *et al.*, J. Physics B **33**, 2753 (2000)
[24] Docenko O. *et al.*, J. Phys. B **39**, S929 (2006)
[25] Pashov A. *et al.*, Phys. Rev. A **76**, 022511 (2007)
[26] Fellows C. E. *et al.*, J. Mol. Spec. **197**, 19 (1999)
[27] Korek M. *et al.* , Chem. Phys. **256**, 1 (2000)
[28] Derevianko A., Babb J. F. Dalgarno A., Phys. Rev. A **63**, 052704 (2001)
[29] Aymar M. Dulieu O., J. Chem. Phys. **122**, 204302 (2005)

[30] Kotochigova S. Tiesinga E., J. Chem. Phys. **123**, 174304 (2005)

[31] Byers Brown W. Whisnant D. M., Chem. Phys. Lett. **7**, 329 (1970)

[32] von Meyenn K., Z. Physik **231**, 154 (1970)

[33] The third Euler angle is not required since rotations around the molecular axis are not taken into account.